MEMOIRS OF GRADUATE SCHOOL OF ENG. *TOKYO METROPOLITAN UNIV.* No. 49, 1999

Failure Mechanism of Reinforced Concrete Interior Beam-Column Joints

Shinji MORITA*, Kazuhiro KITAYAMA** and Akio KOYAMA***

Synopsis

The effects of a column axial load and a beam bar bond within a joint on the shear strength in reinforced concrete interior beam-column joints were investigated by testing cruciform subassemblage specimens. The decrease in the distance between the tensile and compressive forces at a beam critical section due to beam bar bond deterioration within the joint, resulted in the decay of the story shear. The principal compressive strain in a joint panel developed beyond the compressive strain of 0.23 %, which corresponds to the compressive strength obtained using the cylinder test. The joint failed in a shear through compressive collapse of the diagonal concrete strut that was formed in the joint panel. The diagonal joint shear, which could be carried by the surrounding concrete of the diagonal strut, failed in compression. Thus the joint shear does not decrease, even though the joint fails in a shear.

1. Introduction

Several diagonal shear cracks and concrete spalling are observed in a beam-column joint panel of reinforced concrete buildings that have been subjected to severe earthquake motion. This type of joint failure was previously considered to be caused by joint shear. However, Shiohara[1] has proposed that the joint fails due to the increase in flexural compression at the beam critical section that is caused by the bond deterioration along beam bars within the joint. Therefore, the failure mechanism of an interior beam-column joint was investigated by testing six plane cruciform subassemblage specimens.

2. Outline of the Test

2.1 Specimens

Properties of specimens are listed in Table 1. Section dimensions and reinforcement details are shown in Fig.1. Six one-half scale interior beam-column joint specimens were tested. Section dimensions and the specified concrete strength (18 MPa) were common for all specimens.

* Graduate Student, Department of Architecture and Building Science

** Associate Professor, Department of Architecture and Building Science

*** Assistant Professor, Department of Architecture and Building Science, Meiji University

Table 1 Properties of specimens

Specimen	No.1	No.2	No.3	No.4	No.5	No.6
(a) Beam						
Top (Bottom) Bar	4-D25	4-D25	4-D25	4-D25	7-D16	7-D16
at (mm2)	2028	2028	2028	2028	1393	1393
p_t(%)	2.62	2.62	2.62	2.62	1.89	1.89
Stirrups	4-D10	4-D10	4-D10	4-D10	4-D10	4-D10
@(mm)	60	60	60	60	60	60
p_w(%)	1.90	1.90	1.90	1.90	1.90	1.90
Spiral Steel	none	none	none	exist	none	none
(b) Column						
Total Bars	16-D22	16-D22	16-D22	16-D22	16-D22	16-D22
a_g(mm^2)	6192	6192	6192	6192	6192	6192
p_g(%)	1.78	1.78	1.78	1.78	1.78	1.78
Hoops	4-D10	4-D10	4-D10	4-D10	4-D10	4-D10
@(mm)	60	60	60	60	60	60
p_w(%)	1.36	1.36	1.36	1.36	1.36	1.36
Load (kN)	constant in compression +833	constant in tension -833	varying -833～+833	constant in compression +833	constant in compression +833	constant in tension -833
σ_0(MPa)	+7.20	-7.20	-7.20～+7.20	+7.20	+7.20	-7.20
(c) Joint						
Hoops	2-D10	2-D10	2-D10	2-D10	2-D10	2-D10
sets @(mm)	3@90	3@90	3@90	3@90	3@60	3@60
a_w(mm^2)	428	428	428	428	428	428
p_w(%)	0.45	0.45	0.45	0.45	0.57	0.57

Note : a_t=total area of tensile bar,
p_t=tensile reinforcement ratio,
a_g=total area of longitudinal reinforcement,
p_g=gross reinforcement ratio,
σ_0=column axial stress,
a_w=total area of web reinforcement placed between top and bottom beam reinforcement in the joint,
p_w=lateral reinforcement ratio in a joint.
The lateral reinforcement ratio in a joint was computed as the total area a_w of web reinforcement divided by column width and the distance between the compressive and tensile resultants of section.

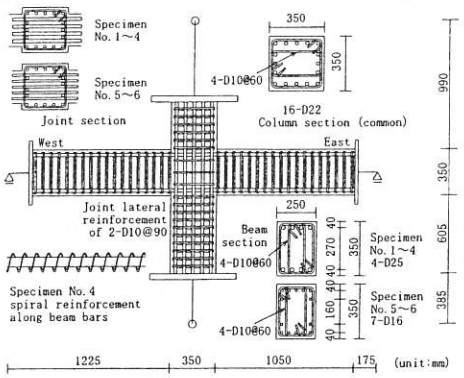

Fig.1 Section dimensions and reinforcement details

The column axial load and beam bar diameter were chosen as the test parameters. The column axial load was as follows; a constant compressive load of +833 kN, a constant tensile load of –833 kN and the varying load from –833 to +833 kN. The beam bar diameter of D16 or D25 was used. The beam longitudinal bars were reinforced by spiral steel of D3 within both joint and hinge regions in Specimen No.4. The joint lateral reinforcement consisted of three sets of 2-D10 for all specimens. Properties of the steel and the concrete are listed in Table 2 and 3.

Table 2 Properties of steel bar

Diameter	Yeild stress σ_y (MPa)	Tensile strength σ_t (MPa)	Elongation ε_u (%)	Young's Modulus E_s (GPa)
D3	305	402	40.2	128
D10	377	643	14.2	181
D16	508	709	16.5	194
D22	548	739	15.1	196
D25	511	668	16.8	194

E_s: Young's Modules was obtained by tensile testing of steel bar

Table 3 Properties of concrete

Specimen	Compressive strength σ_B (MPa)	Strain at σ_B ε_c (%)	Tensile strength σ_t (MPa)	Young's Modulus E_c (GPa)
No.1	22.1	0.248	1.75	19.5
No.2	22.0	0.226	2.28	20.9
No.3	21.5	0.241	1.71	17.8
No.4	22.5	0.221	1.59	19.0
No.5	21.6	0.217	1.71	20.0
No.6	21.7	0.221	1.88	18.9

E_c: Secant modulus at 1/4 σ_B

2.2 Loading Method

The loading apparatus is shown in Fig.2. The beam ends were supported by horizontal rollers,

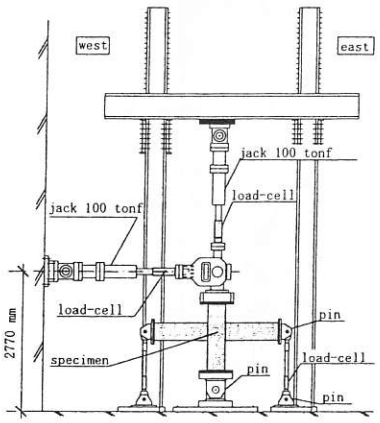

Fig.2 Loading apparatus

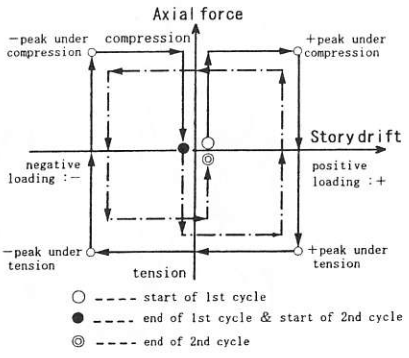

Fig.3 Loading path for Specimen No.3

whereas the bottom of the column was supported by a mechanical hinge. The reversed horizontal load and the column axial load were applied at the top of the column. The column axial load was controlled by the load, and a lateral force was controlled by the story drift angle θ for one cycle of 1/400 radian, two cycles of 1/200, 1/100 and 1/50 radian, one cycle of 1/33 radian and to the end after two cycles of 1/25 radian. In Specimen No.3, either the story drift angle or the column axial load was maintained constant while the other was changed, as shown in Fig.3.

2.3 Instrumentation

The lateral force applied to the top of a column, the column axial load and the shear forces of both beam ends were measured using load-cells. The story drift, deflections of both beams and the upper and lower column, local displacements of the joint panel and the slip of the beam bars at the center of a beam-column joint were measured using displacement transducers, and the strains of beam bars, column bars and the joint lateral reinforcement were measured using strain gauges.

3. Test Results

3.1 General Observations

The crack patterns following the story drift angle of 1/25 radian are shown in Fig.4. Diagonal shear cracks occurred in the joint panel for all specimens. The diagonal crack angle to a beam axis of the specimens that were subjected to the constant column axial load in compression was larger than the specimens that were subjected to the constant column axial load in tension. Concrete spalling was observed in the joint panel for the specimens that were subjected to the compressive column axial load. More diagonal cracks occurred in the joint panel of Specimen

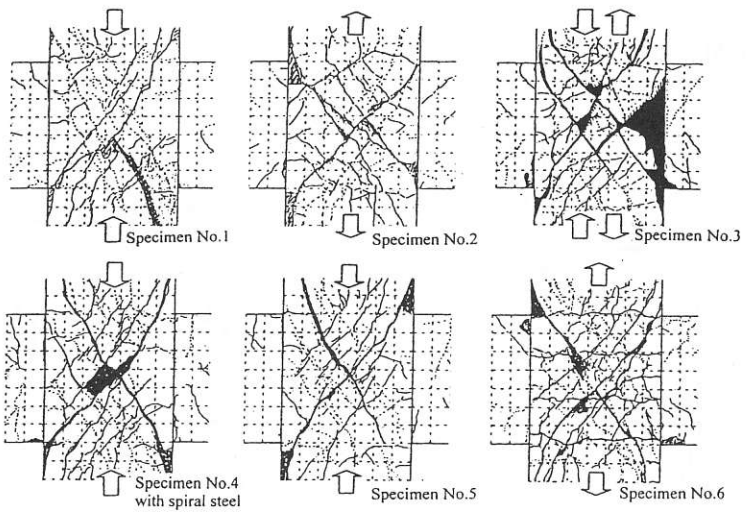

Fig.4 Crack patterns

No.3 when the specimen was subjected to the tensile column axial load than when the specimen was subjected to the compressive column axial load. The stress in a few beam and column bars reached yield stress at the story drift angle of 1/25 radian for all specimens. Therefore, it was judged that neither the beam nor the column yielded. The strain distributions of the joint lateral reinforcement at the maximum story shear force are shown in Fig.5. These strains exceeded the yield strain at the maximum story shear force for all specimens. The contributions of the beam and column deflections and the joint shear distortion to the story drift are shown in Fig.6 for Specimens No.1 and 6. The deflection of beams and columns shared approximately 60 to 90 % of the total story drift before reaching the maximum story shear force. However, the contribution of the joint shear distortion became large and exceeded the half of the total story drift after reaching the maximum story shear force. Therefore, all specimens eventually failed in joint shear, regardless of the column axial load or the beam bar bond condition.

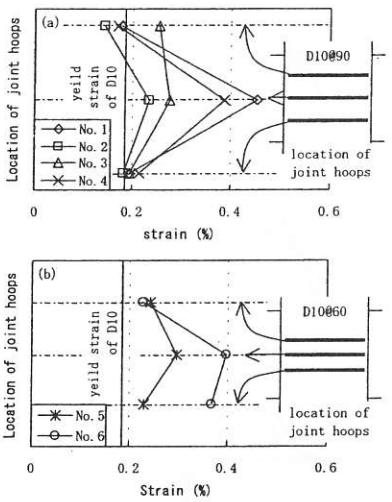

Fig.5 Strain distribution of joint lateral reinforcement

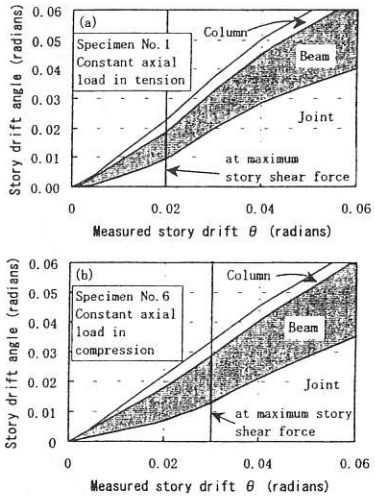

Fig.6 Components of story drift

3.2 Story Shear Force – Drift Relationships

The story shear force – drift relationships are shown in Fig.7. The initial stiffness of Specimen No.1, which was subjected to the constant column axial load in compression and had a beam bar diameter of D25, was larger than that of Specimen No.2, which was subjected to the constant column axial load in tension. This is due to the increase in the bending moment on columns under the compressive column axial load. The story shear force of Specimen No.2, which was subjected to the constant column axial load in tension and had a beam bar diameter of D25, decreased to 0.94 times that of Specimen No.1. The story drift at the maximum story shear force of Specimen No.2 was larger than that of Specimen No.1. The specimens subjected to the constant column axial loads in compression or tension having a beam bar diameter of D16 (Specimens No.5 and 6) showed the same hysteresis characteristics as specimens for which the beam bar

diameter was D25. Therefore, the column axial load is thought to have affected both the hysteresis characteristics and the story shear strength for beam-column subassemblages. The hysteresis characteristics were very similar among the specimens that were subjected to the same column axial load, independently of beam bar diameter. The maximum story shear force of Specimen No.4, in which the beam longitudinal bars within the joint were reinforced by spiral steel, was larger than that of the other specimens, but the differences were small. The effect of beam bar diameters on the hysteresis characteristics was not observed. For all specimens, the estimation of the story shear capacity at the joint shear strength as computed according to the provisions set forth by Architectural Institute of Japan[2] was conservative compared to the measured story shear.

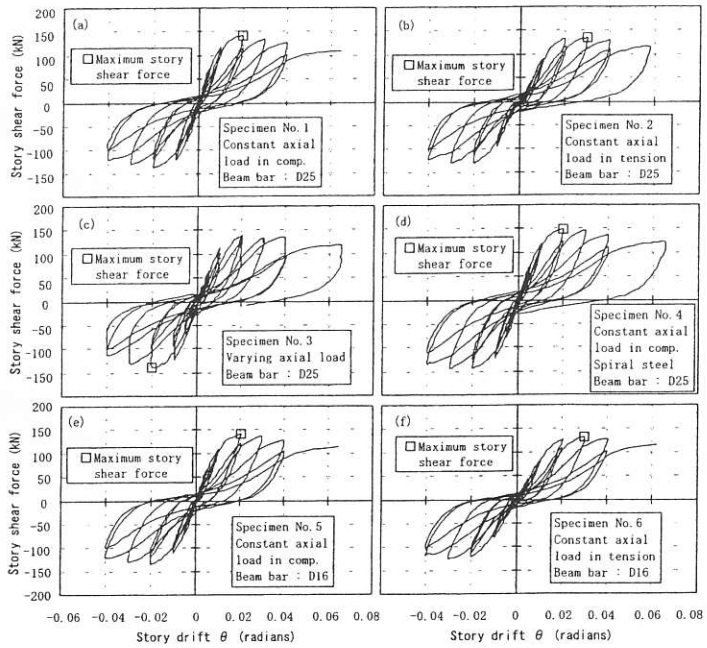

Fig.7 Story shear force - story drift relationships

4. Discussion of Test Results

4.1 Joint Shear Force – Drift Relationships

The joint shear force was computed using the two methods described in the following. a) The tensile force of the beam bars was computed by dividing the beam bending moment on the critical section by a constant lever arm length. The joint shear force is obtained using the following equation:

$$V_j = \frac{M_b}{j_b} + \frac{M_b'}{j_b'} - V_c \tag{1}$$

where M_b and M_b' are the beam bending moments on the critical sections, j_b and j_b' are the lever arm lengths on the beam critical section, and V_c is the measured story shear force. The lever arm lengths j_b and j_b' are constant and are equal to 7/8 the effective depth of the beam section. b) The tensile force of the beam bars was computed directly from the beam bar strain that was measured using strain gauges at the critical section. The joint shear force was obtained using the following equation:

$$V_j = \Sigma a_t \sigma_s + \Sigma a_t' \sigma_s' - V_c \tag{2}$$

where a_t and a_t' are the sectional areas of the top and bottom beam bar, σ_s and σ_s' are the stresses of the beam bar on the critical section, as computed using the measured strains in conjunction with the Ramberg-Osgood Model. The joint shear stresses of Specimens No.1 and 6 from Eqs.(1) and (2) are shown in Fig.8. The joint shear stresses were computed by dividing the joint shear force by the effective sectional area of the joint panel that was the product of the average width of the column and beam multiplied by the column depth. The skeleton curve shown in Fig.8 for the joint shear force was computed using Eq.(2). Equation(1) is generally used for this calculation. The joint shear stresses obtained using Eq.(1) decreases after the peak of the story shear force. In contrast, the joint shear stresses obtained using Eq.(2) increases to the end of the test. The relationships between the joint shear stresses obtained from normalized Eq.(2) for concrete compressive strength, σ_B, and the story drift angles at the peaks of each cycle are shown in Fig.9. Since the joint shear stresses increase successively for all specimens, the joint shear did not contribute to the decrease in the story shear force.

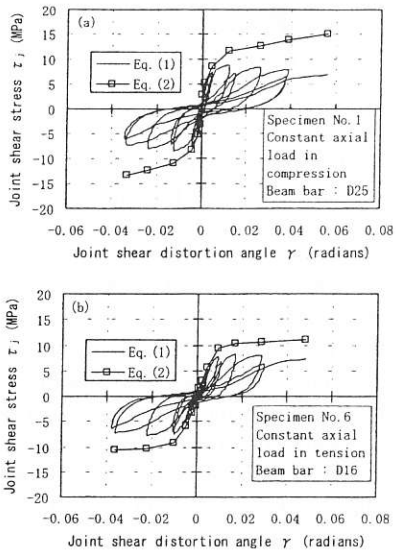

Fig.8 Joint shear stress - joint shear distortion relationships

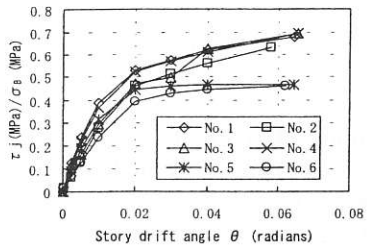

Fig.9 Normalized joint shear stress - story drift relationships

4.2 Beam Bar Bond

The beam bar stress – story drift angle relationships for Specimens No.1 and 6 are shown in Fig.10. The bond stresses along a beam bar within a beam-column joint for all specimens are shown in Fig.11. The average bond stress along the beam bars within a joint was computed using the difference between the beam bar forces at opposite column faces. Beam bar diameters had only a small effect on the beam bar bond stress before reaching the story drift angle of approximately 1/50 radian. The bond stresses of specimens subjected to the compressive column axial load were larger than those of the specimens subjected to the tensile column axial load. The bond stress along the beam reinforcement within a joint decreased after the stress reached the bond strength, even though the tensile force in beam bars at the beam critical section increased successively. Thus, the bond deterioration along beam bars is thought to have occurred within the joint.

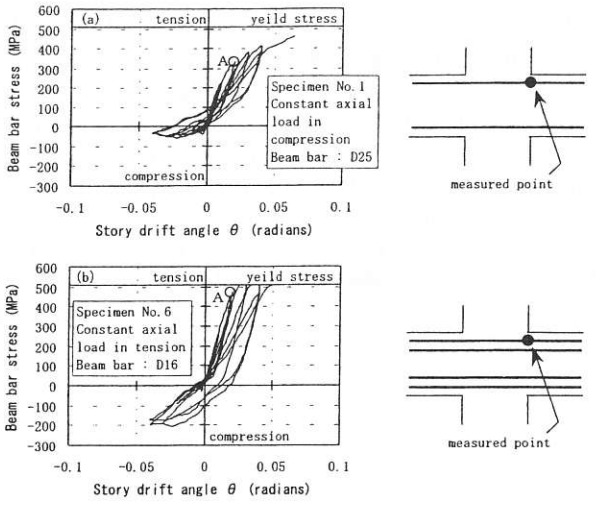

Fig.10 Beam bar stress - story drift relationships

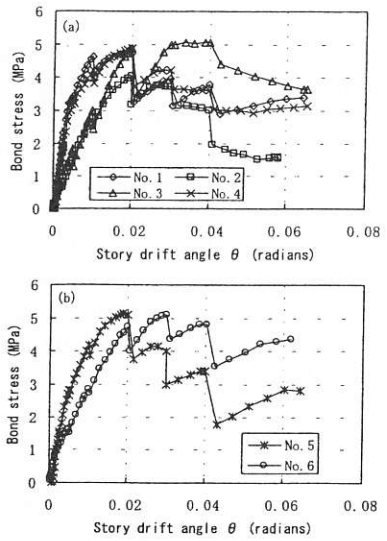

Fig.11 Bond stress along beam bar within joint – story drift relationships

4.3 Column Bar Bond

The Column bar stress on the upper critical section of the joint – story drift angle relationships is shown in Fig.12. In this figure, the column bar stress was omitted after six cycles (θ = 1/50 radian), because the accuracy of the measured strains was unclear. The column bar stress at the column critical section reversed from the compression to tension, as shown by arrows in Fig.12, after the joint shear crack occurred, even though the tensile column bar stress at the opposite critical section increased successively. Thus, the column bar bond is thought to have deteriorated within the joint. The inclination of the diagonal resultant force in the joint panel as computed by dividing the vertical joint shear obtained from the column bar stresses by the horizontal joint shear tended to become approximately 45 degrees. The inclination of the resultant compressive force coincides approximately with that of the compressive principal strain.

4.4 Lever Arm Length

The bond deterioration along beam bars within the joint caused the increase in the compressive resultant force on the beam critical section. As a result, the lever arm length of coupled forces on the beam critical section decreases. The change in lever arm length on the beam critical section is shown in Fig.13. The lever arm length, j_b, was computed by dividing the beam bending moment on the critical section by the tensile force of the beam bars. The lever arm length had a tendency to decrease from 7/8d (d: effective depth of a beam section) for all specimens. The stiffness in the beam bar stress – strain relationship decreased suddenly at point A, as shown in Fig.10, whereas the tensile force of beam bars increased to the end of the test. Therefore, the decrease in the bending moment on the beam critical sections resulted in the decay of the story shear force.

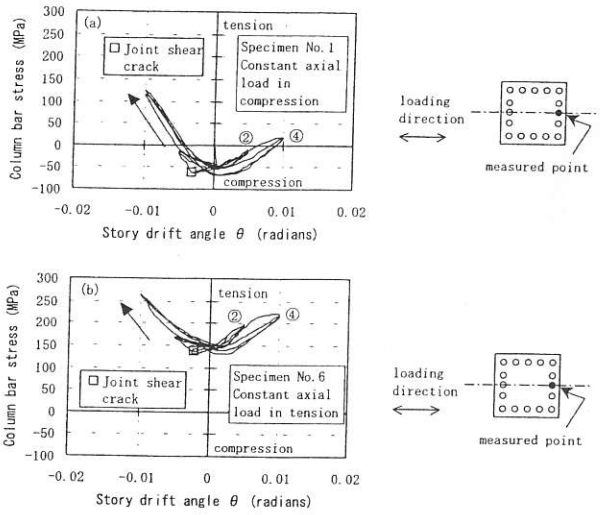

Fig.12 Column bar stress - story drift relationships

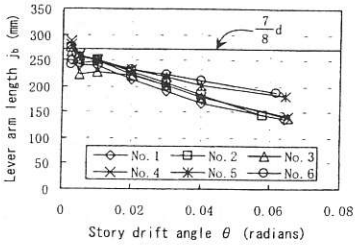

Fig.13 Change in lever arm length

4.5 Principal Strain in the Joint Panel

The tensile principal strain – compressive principal strain relationships are shown in Fig.14. The direction of the compressive principal strain to the beam axis for Specimens No.1 and 6 are shown in Fig.15. The principal strains in the joint panel were computed using average strains measured by two sets of horizontal, vertical and diagonal displacement transducers, respectively. The compressive and tensile principal strains increased as the cyclic loading progressed. The stiffness of the joint shear force obtained using Eq.(2) decreased remarkably in the joint shear force – drift relationships, as shown in Fig.8. The joint shear distortion increased abruptly because of the increase in the principal strains. The compressive principal strain exceeded the strain of 0.23% at the concrete compressive strength. Therefore, the joint failed in shear through compressive collapse of the diagonal concrete strut that was formed in the joint panel. The diagonal joint

shear, which could be carried by the surrounding concrete of the diagonal strut, failed in compression, as shown in Fig.16. Thus the joint shear does not decrease, even though the joint fails in shear. The direction of compressive principal strain increased as the cyclic loading progressed and eventually reached approximately 60 degrees.

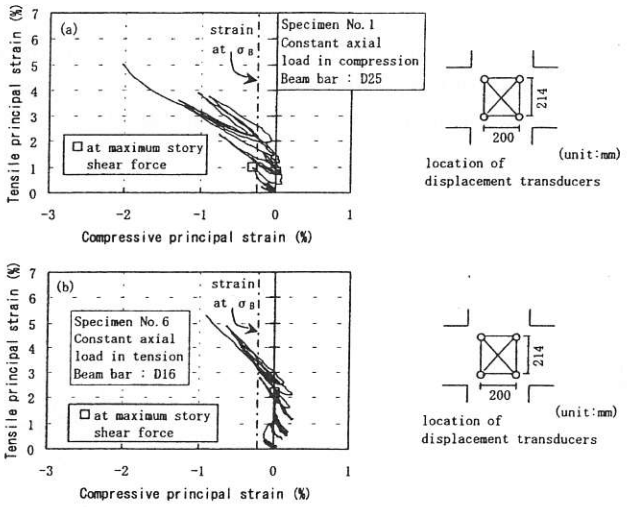

Fig.14 Tensile principal strain – compressive principal strain relationships

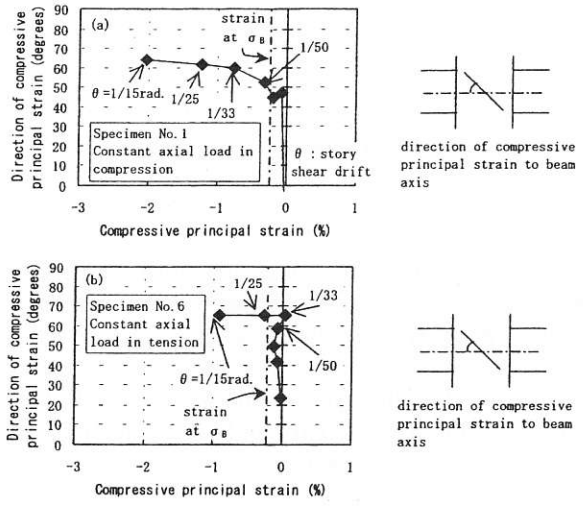

Fig.15 Direction of compressive principal strain

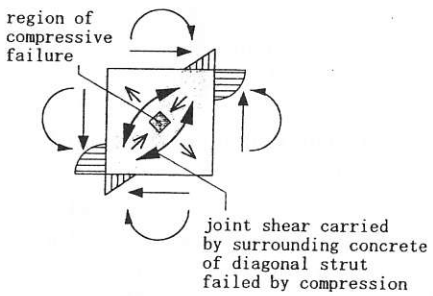

Fig.16 Stress transmission in joint panel

5. Conclusions

The finding of the present study can be summarized as follows:

(1) The column axial load affected the story shear strength for beam-column subassemblages. For all specimens, the estimation of the story shear capacity at the joint shear strength computed according to the provisions by Architectural Institute of Japan[2] was conservative compared to the measured story shear.

(2) The joint shear stresses obtained by Eq.(2) increased to the end of the test, whereas the story shear force decrease following the maximum story shear force. The decrease in the beam bar bond stress within the joint was caused by bond deterioration.

(3) The stiffness of tensile beam bar stress decreased suddenly at point A, as shown in Fig.10, whereas the tensile force of beam bars increased to the end of the test. The decrease in the bending moment on the beam critical sections resulted in the decay of the story shear force.

(4) The column bar bond deteriorated within the joint following joint shear cracking. The inclination of the diagonal resultant force in a joint panel as computed by dividing the vertical joint shear by the horizontal joint shear tended to become approximately 45 degrees. The inclination of the resultant compressive force coincided approximately with that of the compressive principal strain.

(5) The stiffness of joint shear force obtained using Eq.(2) decreased suddenly in the joint shear force – drift relationships. The joint shear distortion increased abruptly because of the increase in the principal strains. The diagonal joint shear, which could be carried by the surrounding concrete of the diagonal strut, failed in compression. Thus the joint shear does not decrease, even though the joint fails in shear.

References:

1) Shiohara, H., et al., "Re-evaluation of Joint Shear Tests of R/C Beam-Column Joints Failed in Shear", Proceedings of the Japan Concrete Institute, Vol.19, No.2, pp.1005-1010, 1997 (in Japanese).

2) Architectural Institute of Japan, "Design Guidelines for Earthquake Resistant Reinforced Concrete Buildings Based on Inelastic Displacement Concept (Draft)", 1997.